Physicochemical properties of chitosan–magnetite nanocomposites obtained with different pH

Christian Chapa González[1] ⑩**, Javier Ulises Navarro Arriaga[2] and
Perla Elvia García Casillas[2]**

Abstract

The physicochemical properties of the nanoparticle surface determine the performance of nanocomposites in biomedical applications such as their biodistribution and pharmacokinetics. The physicochemical properties of chitosan, such as apparent charge density and solubility, are pH dependent. Similarly, Fe_3O_4 nanoparticles are susceptible to variations in their physicochemical properties due to changes in pH. In this work, we evaluated the physicochemical properties of chitosan–magnetite nanocomposites that were suspended at pH 7.0, 9.0, and 11.0 to determinate the effect on particle size, zeta potential, and mass percentage of the polymeric coating, in addition to the crystalline phase and magnetic properties of magnetite phase. X-ray diffraction results exposed that the present phase was magnetite with no other phases present and that the crystallite size was between 10.8 and 14.1 nm. Fourier transform infrared verified the chitosan functional groups in treated samples while the percentage of mass determined by TGA found to be nearly 9%. Scanning electron microscopy micrographs corroborated the spherical shape of the bare and chitosan-coated nanoparticles. Dynamic light scattering results showed that chitosan coating modifies the zeta potential, going from a potential of -11.8 mV for bare particles to -3.0 mV (pH 11). Besides, vibrating sample magnetometer measurements showed that coercivity remained very low, which is desirable in biomedical applications.

Introduction

Chitosan (CS), deacetylated chitin or poly (D-glucosamine) is a linear polysaccharide derived from Chitin. The obtention methods of this polymer include alkaline hydrolysis and thermochemical treatment. Chitosan is composed of randomly distributed β-(1-4)-linked D-glucosamine (GLcN) and N-acetyl-D-glucosamine (NAG). Thus, the occurrence of primary amino groups on the units of GlcN of its backbone gives chitosan a cationic character, or positive charge on its surface, at neutral/physiological pH. In fact, the apparent pKa fluctuates between 6.3 and 6.8 when the degree of acetylation is <70% and CS becomes soluble in a medium with pH ≤ 5.0.[1] CS and derivatives exhibit biocompatibility and they are suitable for several possible biomedical applications including functionalization or coating of magnetic nanoparticles.[2–9]

At present, magnetite nanoparticles (MNP) are under intense investigation for clinical applications. Magnetite nanoparticles are susceptible to pH, both in the synthesis process by co-precipitation and in post-synthesis treatments. It has been shown that pH values ranging 9.7 to 10.6 tend to produce pure magnetite with no other iron oxide. Other products, such as goethite and maghemite tend to be found when the synthesis is performed in pH below 8.5.[10] Likewise, it has been shown that the saturation magnetization is modified with the different pH values maintained during the synthesis of the particles[11] and pH value affected the surface zeta potential of Fe_3O_4 nanoparticles. It has been demonstrated that magnetite nanoparticles possess relatively high negative and positive zeta potentials (up to 40 mV) below and above the isoelectric point, respectively.[12]

The chitosan–magnetite nanocomposites serve several purposes including physicochemical stability, regulated delivery of drugs, increased interaction with cells and tissues, and improvement in the bioavailability or efficacy of drugs. Steric repulsion and electrostatic repulsion are the key forces required for better stability of magnetite nanoparticles when they are obtained by

[1]Biomedical Engineering, Institute of Engineering and Technology of the Autonomous University of Juarez Cityl, Cd. Juarez, Mexico
[2]Department of Physics and Mathematics, Institute of Engineering and Technology of the Autonomous University of Juarez City, Cd. Juarez, Mexico

Corresponding author:
Christian Chapa González, Universidad Autonoma de Ciudad Juarez, Avenida Plutarco Elias Calles 1210, Chihuahua, Mexico.
Email: christian.chapa@uacj.mx

methods like co-precipitation. CS and other materials have been employed as coatings to obtain improved colloidal stability and other interesting properties in the biomedical area.[13-15] It is well known that pH-dependent properties of CS influence its biomedical activity and potential applications of the nanocomposites. Furthermore, polymers, such as CS, have been shown to improve the action of anticancer drugs in nanocomposites formulations.

Recent advancement in nanocomposites obtention has made the possibility to prepare CS nanometer-size materials with controlled structure. In the literature, there are some attempts to evaluate the influence of the pH in CS-coated MNP. The studies are mainly emphasized on drug release determination at pH 5.0 and 7.4,[16] pH 5.5, 7.4, and 9.8,[17] and pH 5.3 and 7.4,[18] where the highest cumulative release is obtained under acidic conditions. However, there are many challenges associated with the process of controlling the parameters of synthesis of the CS-magnetite nanocomposites, such as determining the amount of the coating by controlling the pH during the synthesis.

Herein, we report the effect of pH on size distribution, zeta potential, and mass percentage of the coating of CS-coated nanocomposites prepared by a simple, non-time-consuming, and reproducible method. During the synthesis of magnetite by alkaline co-precipitation, it is common to carry out several washes with distilled water, which lowers the pH. Therefore, studies were conducted by mixing the polymer solution with a suspension of magnetite nanoparticles that, by washing with distilled water, has reached pH 11.0, 9.0, and 7.0. We do not involve acidic conditions in nanoparticle synthesis to avoid phase mixing of iron oxides such as maghemite and γ-Fe_2O_3.

Experimental

Preparation of magnetite- (Fe_3O_4) and chitosan-coated magnetite nanocomposites

Nanocomposites were synthesized as previously described.[14,19] The synthesis was carried out by means of the co-precipitation reaction, in which a stoichiometric ratio of 2 to 1 with respect to the Fe^{3+} and Fe^{2+} ions is preserved. First, 100 mL of 0.1 M ferric chloride ($FeCl_3$) and 0.5 M ferrous sulfate ($FeSO_4$) were prepared separately and both solutions were mixed with vigorous stirring for 15 min. Second, an excess of ammonium hydroxide solution (NH_4OH, 30%) was put into the mixture, until a dark precipitate formed. The reaction was kept under stirring for 30 min and the pH was measured. Then, the precipitate was collected by decantation using a permanent magnet; the supernatant was discarded and immediately washes were carried out with distilled water. The sample was centrifuged at 3000 r/min for 5 min between each wash. The pH was adjusted with 0.1 M HCl or 0.1 M NaOH as required. Finally, three different suspensions with pH 11.0, 9.0, and 7.0 were labeled and separated in two equivalent volumes, one volume for characterization of the uncoated material and the other for the immediate CS coating procedure which is described below.

To obtain CS-coated nanocomposites, the preparation of a CS solution in an aqueous acid solution is required.[9] CS (medium molecular weight) was provided by Sigma-Aldrich and used without further purification. 25 mL of CS solution was prepared dissolving 0.05 g in 2% acetic acid mechanically stirred for 40 min, in a room temperature glass. The aqueous suspension of MNP was poured into the CS solution and kept stirring for 1 h; the same procedure was carried out with the magnetite suspensions at determined pH. The precipitate was collected by magnetic decantation while the supernatant was discarded. The resulting magnetic material was washed three times with 10 mL of distiller water and with 10 mL of ethanol (70%). The product was dried at 80°C in the oven for 24 h. After drying, the samples were collected in vials for further characterizations.

Characterization

X-ray diffraction (XRD) was employed to verify the structure of pure magnetite nanoparticles. X-ray diffraction was performed using a PANalytical X´Pert MRD PRO X-ray diffractometer, for analyzing the crystalline phases of Fe_3O_4 samples whose pH was established in the synthesis procedure. XRD diffraction patterns were obtained using copper-monochromatized Kα1 radiation, under 40 kV and 30 mA. In this way, it was also possible to calculate the crystallite size using the Scherrer formula.[20]

The size distribution and morphology of the CS-coated nanocomposites were analyzed by scanning electron microscopy (SEM) using a JEOL JSM-7000f apparatus operating at 15–20 kV. The samples were dispersed on a carbon conductive tape before SEM observation. Diameter of 100 individual nanoparticles was measured directly from the images using the line tool of the equipment software to provide measures for the size distribution of all samples. The results are presented as mean ± SD. Furthermore, mean particle size was determined by dynamic light scattering (DLS) in triplicate using a Nanotrac Wave Particle Size Analyzer (Microtrac). At the same time, the zeta potential of each sample was measured. The measurements were made after suitable dilution of the aqueous particle suspensions, in order to characterize the surface adsorption of CS on the MNP, the z values of the non-coated (blank) nanoparticles and of the CS-coated MNP were compared.

The CS bounded to the MNP was evaluated by Fourier transform infrared (FTIR) spectrometry with attenuated total reflection (ATR) (Thermo Scientific Nicolet 6700 spectrometer). The IR spectra, range from 4000 to 600 cm^{-1}, were obtained with a resolution of 4 cm^{-1} The most important bands of CS and CS-coated nanoparticles have been identified by comparison with previously published data. Thermogravimetric analysis of CS-coated MNP was accomplished on a TA Instruments (DSC-TGA, SDT Q600) analyzer at a heating rate of 10°C min^{-1} from ambient to 700°C under a nitrogen purge (50 mL min^{-1}). This analysis was performed to determine the effect of pH on the amount of CS incorporated on the MNP surface.

The magnetic properties of MNP before and after CS-coating were analyzed by using a vibrating sample magnetometer (Versalab, Quantum Design) at room temperature with a H_{max} of 10 kOe.

Results and discussion

The process of synthesis of magnetite by chemical precipitation involved the addition of NH_4OH, whereby a pH of 13.0 was reached. This procedure was performed in triplicate to reach the pH of interest in each sample. Once dried, the diffraction patterns shown in Figure 1 were obtained. The XRD diffractograms of all samples, magnetite pH 11, magnetite pH 9, and magnetite pH 7 are shown. The sites and intensity of the XRD peaks (2 2 0), (3 1 1), (4 0 0), (4 2 2), (5 1 1), and (4 4 0) are consistent with the JCPDS Ref. Pattern: Magnetite, 01-075-0449. It is well known that Fe_3O_4 has a cubic inverse spinel structure with oxygen forming an fcc closed packing, while Fe cations occupy the interstitial octa- and tetrahedral sites and the pH can influence a phase change;[21] it would be reflected in a different crystalline structure, which would affect its magnetic properties and, ultimately, its biomedical application combined with CS. It can be noticed that the Fe_3O_4 nanoparticles synthesized and washed to the indicated pH has no additional peaks corresponding to other phases of iron oxides. X-ray diffraction analysis shows that a single-phase cubic spinel structure is present in all the samples. However, it can be noted that the intensity of the 2θ 30.362° diffraction peak has slightly decreased at increasing pH. This slight decrease in the diffraction peak can be attributed to the fact that in alkaline pH the high concentration of hydroxyl groups leads to the formation of secondary phases. Goethite (αFeOOH) formation has been demonstrated in prolonged reaction times at alkaline pH.[22] In the same way, it has been found that the number of washes and the resuspension of nanoparticles in distilled water promote the formation of Fe_3O_4 in the precipitation method.[23]

In addition to checking the crystalline phase of the precipitate obtained, the XRD patterns were used to estimate the crystallite size of each sample. The Scherrer equation (1) (also referred to as the Debye–Scherrer equation) relates the full-width at half-maximum (FWHM) of a powder diffraction peak to the dimensions of crystallites in a powder.

$$D = \frac{K\lambda}{\beta\cos\theta} \tag{1}$$

where D is the crystallite size, K is the Scherrer's constant, which usually about 0.9,[24-25] depends on whether the FWHM or the integral width is chosen and it also shows the shape of crystal and size distribution, θ is the Bragg angle between the incident ray and the diffracted plane, and β is the FWHM of the peak. The most intense peak is observed at (3 1 1) in all samples. In this way, such data were used to perform the calculations. The sizes of crystallites of uncoated magnetite were found to be 10.8, 12.1, and 11.0 nm of samples suspended at pH 7.0, 9.0, and 11.0, respectively.

Once the one-step procedure for nanoparticle coating was carried out, the dried samples were analyzed by FTIR to corroborate the functional groups of the chitosan on the magnetite nanoparticles' surface. Figure 2(a) and (b) exhibit the FTIR spectra of CS and CS-coated nanocomposites at pH 9. As shown in Figure 2(a), the FTIR spectrum of CS shows strong characteristic bands located in the range between 3400 cm^{-1} and 3200 cm^{-1} corresponding to combined bands of hydroxyl bonds[26] and primary amines,[27] while 1557 cm^{-1} band is attributed to carbonyl asymmetric stretching vibrations, and C-O stretching vibrations of the pyranose ring at 1002 cm^{-1}.[28] Comparing with CS, a noticeable change is apparent in the spectra of CS-coated samples. Comparing with CS, a noticeable change is apparent in the spectra of CS-coated samples. Fourier transform infrared spectra of the CS-coated system (Figure 2(b)) indicate decreased band intensities. It is possible to see a deep peak at about 500 cm^{-1} characteristics of the Fe-O bond absorption. This confirms the presence of the magnetic core. Moreover, it can be observed that the bands around 3240 and 1002 cm^{-1} are present in Figure 2(b) indicating the presence of
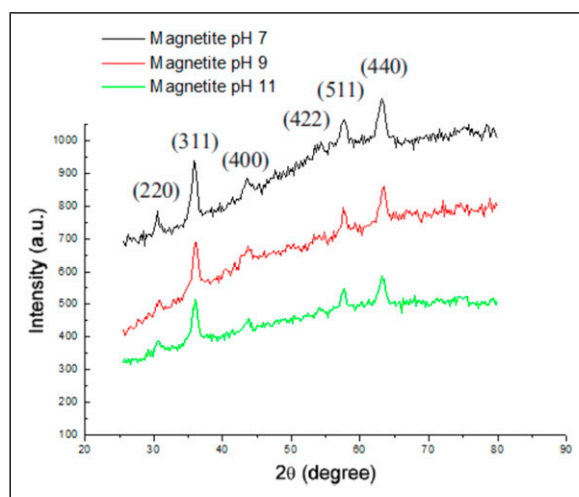

Figure 1. X-ray diffraction profiles of samples synthesized and resuspended at pH 7.0, 9.0, and 11.0.

the chitosan shell. The absorption band at about 500 cm^{-1} is most likely due to Fe-O. The absorption band at about 500 cm^{-1} is most likely due to Fe-O symmetrical stretching vibration[29] that is in a good accordance with previously published paper.[30] There were no significant variations in the IR spectra from the samples in the other two pH. It can be stated that the proposed procedure of coating Fe_3O_4 nanoparticles with CS in a single step was effective regardless of the pH at which the suspension of nanoparticles was maintained.

To investigate the morphology and size of the uncoated and CS-coated nanocomposites, SEM images have been registered. There are no noticeable differences in the morphology of uncoated and coated nanoparticles at different pH values. SEM images show the spherical shape of Fe_3O_4 nanoparticles (Figure 3). The average size (diameter) of uncoated nanoparticles was 12.9 ± 1.9 nm, 21.6 ± 2.8 nm, and 21.4 ± 2.8 nm in the case of samples with pH 7.0, 9.0, and 11.0, respectively. Likewise, the CS-coated nanoparticles retained their spherical morphology and the mean diameter was 77.7 ± 3.6 nm, 83.7 ± 7.3 nm, and 90.5 ± 6.3 nm for the samples with pH 7.0, 9.0, and 11.0, respectively. It can be noted that there was an increase in the mean size of coated nanoparticles (Figures 4(a) and (b)). The addition of CS to the nanoparticle suspension causes agglomerates and there is a tendency for the size of these agglomerates to increase with the higher pH in the suspension. This is attributed to the fact that, in a more alkaline environment, the surface of the magnetite nanoparticles has a more negative charge which enables greater interaction with protonated amine groups in the CS solution. To corroborate this, the zeta potential of the samples was measured, and the hydrodynamic size was determined at the same time.

The impact of the one-step method of CS-coating on the electrokinetic potential and hydrodynamic size of magnetite nanoparticles, obtained by co-precipitation, resuspended in a pH interval (7–11) was studied. The isoelectric point (IEP), pH of zero electrokinetic potential, has been previously reported as 6.35,[31] 6.6,[12] and 6.8 [32] for Fe_3O_4 synthetized by co-precipitation technique. Therefore, above a pH of 6.8 the net charge for magnetite is negative as can be seen in Table 1. These results were in agreement with previous zeta potential determinations on magnetite.[14] In alkaline media, magnetite is negatively charged as a result of rising accumulation of OH on the surface. When CS solution has been poured to the nanoparticle suspension, the chitosan molecules have immobilized on the surface of the nanoparticles causing the surface potential to increase (Table 1). Studies have demonstrated that only protonated soluble chitosan in its uncoiled configuration is found in acidic pH.[33] Moreover, in Ref. 34, it is proposed that when the pH is increased, the CS adopts a coiled configuration but still retains a percentage of protonated amino groups. This allows the interaction of the CS with the MNPs negative surface to form the coating. In consequence, the zeta potential changes indicated the effective and complete intercalation of CS chains into MNPs surface. CS-coated MNP displayed a less negative charge because of formation of CS layers on the MNP surface. Due to the very different z values of the uncoated and CS-coated MNP, the electrokinetic potential measurement was successfully utilized for qualitatively verifying the coating effectiveness of the CS in the surface of MNP. At the same time, adsorption of CS gives a larger hydrodynamic size of MNP. Table 2 shows a comparison of the estimated size with the different techniques employed, both for uncoated MNP and for CS-coated MNP.

Furthermore, TGA was carried out in order to estimate the quantity of CS adsorbed or immobilized on the magnetite nanoparticles surface and the results are depicted in Figure 5. From the thermogravimetric results, it can be observed that the TG curve is a smooth curve with only one weight loss step. In the literature, it has been reported that the thermal degradation of chitosan in nitrogen is a one-step reaction.[35] For CS-coated nanoparticles, the significant weight loss occurs between 250°C and 300°C associated with the thermal degradation of the chitosan adsorbed on the MNP surface. From the percentage weight loss in the TGA curves of CS-coated magnetite nanoparticles, the amount of chitosan coated on the Fe_3O_4 nanoparticles was
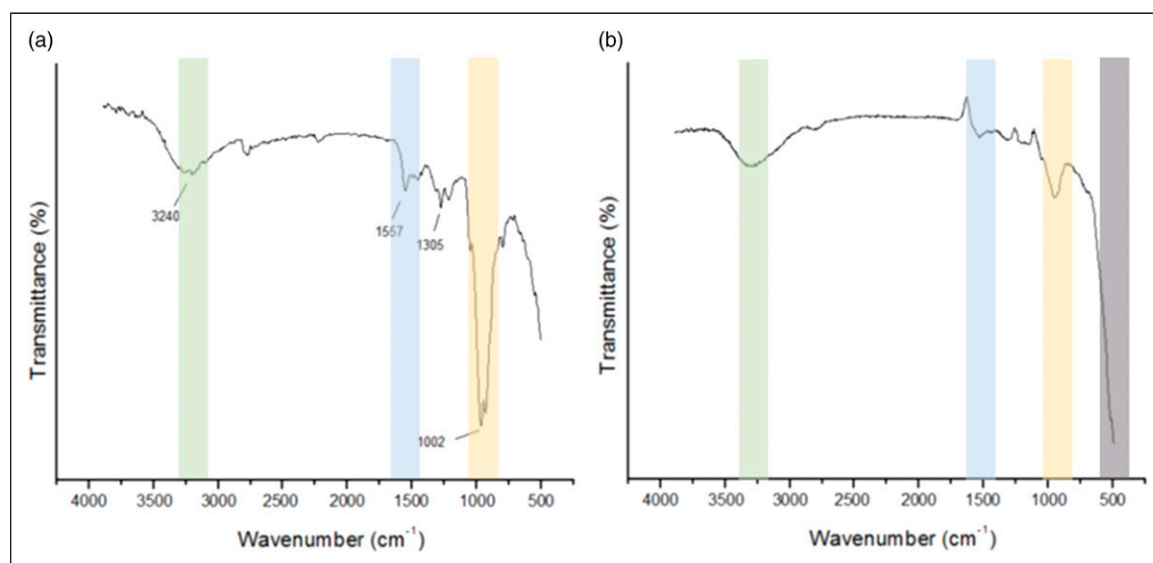

Figure 2. Fourier transform infrared profiles of samples (a) chitosan and (b) CS-coated magnetite nanoparticles. The samples correspond to the one-step method that was carried out with the suspension at pH 9.0.
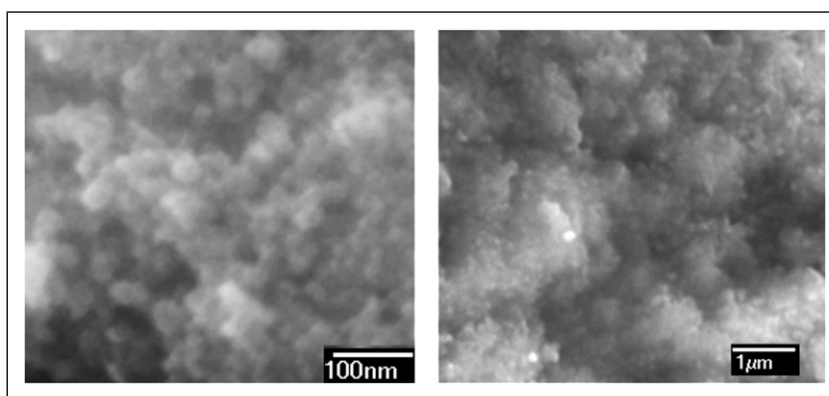
Figure 3. Scanning electron microscopy micrographs of uncoated magnetite nanoparticles sample corresponding to suspension at pH 7.0.
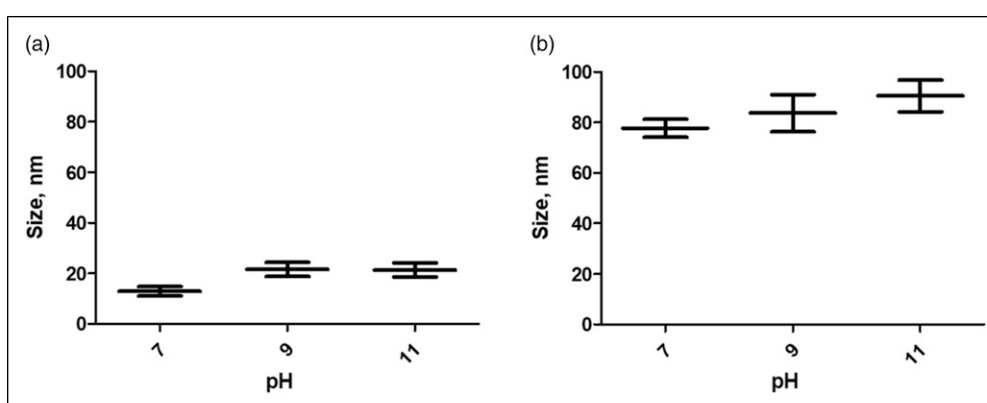

Figure 4. Comparison of the mean size of nanoparticles (a) uncoated magnetite nanoparticles (M) and (b) CS-coated MNP (M-CS), mean ± SD. CS: Chitosan; MNP: magnetite nanoparticles.

Table 1. Electrokinetic (zeta) potential of uncoated and CS-coated Fe_3O_4 nanoparticles.

pH	Zeta potential of MNP, mV	Zeta potential of CS-coated MNP, mV
7.0	−6.5	−2.7
9.0	−7.9	−2.8
11.0	−11.8	−3.0

MNP: magnetite nanoparticles.

Table 2. Size estimates of Fe_3O_4 nanoparticles from XRD, SEM, and DLS data. All values are expressed in nm

	Fe_3O_4 nanoparticles			CS-coated Fe_3O_4 nanoparticles		
pH	Crystallite size (XRD)	Size distribution (SEM)	Hydrodynamic size (DLS)	Crystallite size (XRD)	Size distribution (SEM)	Hydrodynamic size (DLS)
7.0	10.8	12.9 ± 1.9	12.12 ± 4.21	12.1	77.7 ± 3.6	16.83 ± 2.29
9.0	12.1	21.6 ± 2.8	8.83 ± 3.03	14.1	83.7 ± 7.3	21.16 ± 3.58
11.0	11.0	21.4 ± 2.8	11.78 ± 6.92	11.0	90.5 ± 6.3	19.13 ± 5.72

XRD: X-ray diffraction; SEM: scanning electron microscopy; DLS: dynamic light scattering.

found to be 9.2%, 7.76%, and 9.98% for the for the samples with pH 7.0, 9.0, and 11.0, respectively. The remaining weight corresponds to the MNP.

The magnetic properties of uncoated and CS-coated nanoparticles were determined via a vibrating sample magnetometer (VSM). The room temperature hysteresis loops are depicted in Figure 6. The saturation magnetization (Ms) of the formulations was pH dependent. The one-step chitosan coating method did not modify the magnetic behavior of the MNP. It is
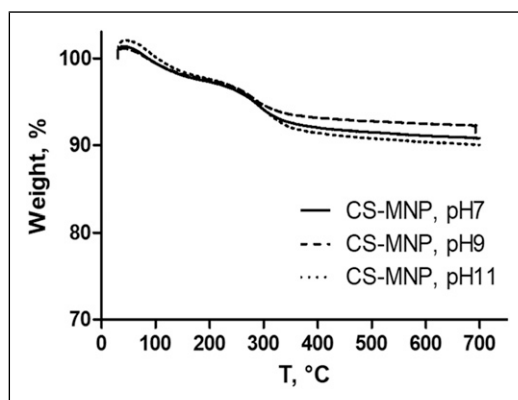
Figure 5. The TGA thermogram curves of particles chitosan-coated magnetite nanoparticles.
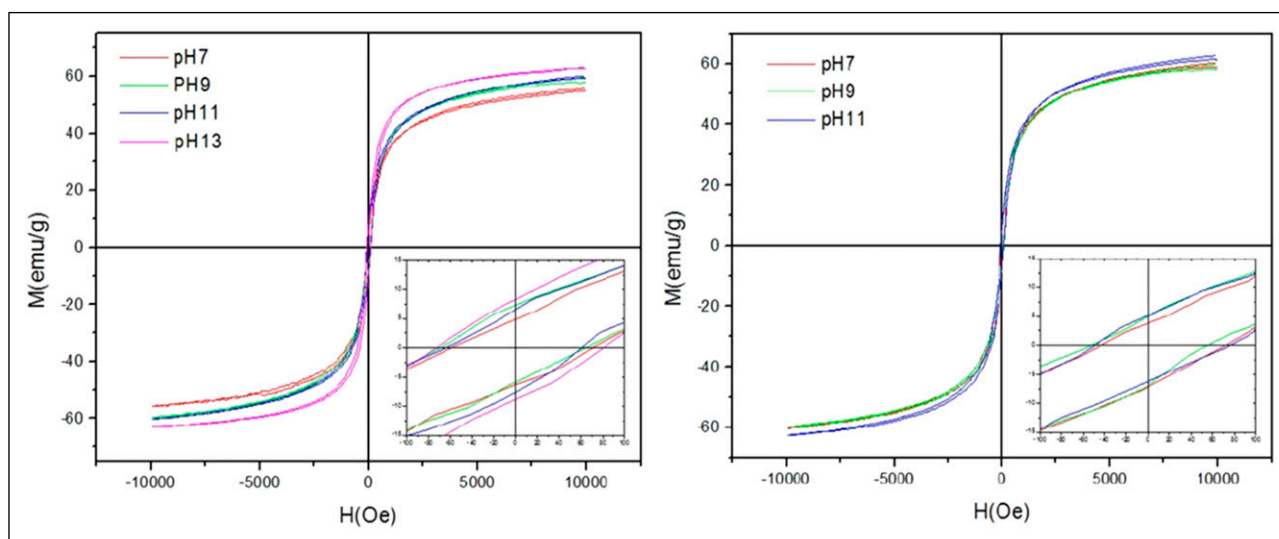

Figure 6. Room temperature hysteresis curves of MNP and CS-coated MNP. MNP: magnetite nanoparticles.

evident that both MNP and CS-MNP showed very low coercivity at room temperature. It should be noted that super-paramagnetic behavior is useful for biomedical applications.[36]

Conclusion

The proposed one-step coating procedure, adding the chitosan solution to the Fe_3O_4 nanoparticle suspensions with various pH values reached after the chemical synthesis by co-precipitation with NH_4OH, was successful. In the proposed procedure, the pH of the suspension does not modify the crystalline phase of MNP, and the coating procedure also does not modify the crystalline phase of Fe_3O_4. The morphology of the nanoparticles remained unchanged throughout the process. Crystallite size is not affected by pH nor by the CS coating. On the other hand, the hydrodynamic size of particles does increase when the CS coating is carried out in the same way as the zeta potential, which demonstrates the effectiveness of the procedure. The amount of coating polymer was found to be about 9% and coercivity remained very low. Even slight physicochemical differences on the nanoparticle surface are reflected in significant biological differences such as pharmacological activity and nanoparticle distribution. For all the above, we have established the effect of pH on the physicochemical properties of the CS coating of magnetite nanoparticles intended for biomedical applications.

Declaration of conflicting interests

The author(s) declared no potential conflicts of interest with respect to the research, authorship, and/or publication of this article.

ORCID iD

Christian Chapa Gonzalez https://orcid.org/0000-0003-1760-6116

References

1. Dragan ES and Dinu MV. Advances in porous chitosan-based composite hydrogels: synthesis and applications. *Reactive Funct Polym* 2020; 146: 104372.

2. Quihui Cota L, Morales Figueroa GG, Valbuena Gregorio E, et al. Membrane of chitosan with essential oils of Romero and Tree of Tea: Potential as biomaterial. *Mex J Biomed Eng* 2017; 38: 255–264.

3. Martel-Estrada SA, Olivas-Armendáriz I, Santos-Rodríguez E, et al. Evaluation of in vitro bioactivity of Chitosan/Mimosa tenuiflora composites. *Mater Lett* 2014; 119: 146–149.

4. Sahranavard M, Zamanian A, Ghorbani F, et al.. A critical review on three dimensional-printed chitosan hydrogels for development of tissue engineering. *Bioprinting* 2020; 17: e00063.

5. Alvarez-Barreto J, Márquez K, Gallardo E, et al. Mesenchymal stem cell culture on composite hydrogels of hydroxyapatite nano-particles and photo-crosslinking chitosan. *Mex J Biomed Eng* 2017; 38: 524–536.

6. Maldonado Lara K, Luna Bárcenas G, Luna Hernández E, et al. Preparation and characterization of copper chitosan nanocomposites with antibacterial activity for applications in tissue engineering. *Mex J Biomed Eng* 2017; 38: 306–313.

7. Irimia T, Ghica M, Popa L, et al. Strategies for improving ocular drug bioavailability and corneal wound healing with chitosan-based delivery systems. *Polymers* 2018; 10: 1221.

8. Li J, Cai C, Li J, et al. Chitosan-based nanomaterials for drug delivery. *Molecules* 2018; 23: 2661.

9. Frank LA, Onzi GR, Morawski AS, et al. Chitosan as a coating material for nanoparticles intended for biomedical applications. *Reactive Funct Polym* 2020; 147: 104459.

10. Andrade ÂL, Souza DM, Pereira MC, et al. pH effect on the synthesis of magnetite nanoparticles by the chemical reduction-precipitation method. *Quím Nova* 2010; 33: 524–527.

11. Ramadan W, Kareem M, Hannoyer B, et al. Effect of pH on the structural and magnetic properties of magnetite nanoparticles synthesised by co-precipitation. *Amr* 2011; 324: 129–132.

12. Szalai AJ, Kaptay G and Barany S. Electrokinetic potential and size distribution of magnetite nanoparticles stabilized by poly(vinyl pyrrolidone). *Colloid J* 2019; 81: 773–778.

13. Reza RT, Martínez Pérez CA, Martínez AM, et al. Study of the particle size effect on the magnetic separation of Bovine Serum Albumin (BSA). *Sen Lett* 2010; 8: 476–481.

14. Chapa Gonzalez C, Roacho Pérez JA, Martínez Pérez CA, et al. Surface modified superparamagnetic nanoparticles: interaction with fibroblasts in primary cell culture. *J Alloys Compounds* 2014; 615: S655–S659.

15. Villegas E, Zavala O, Israel F, et al. Detection of HER2 through antibody immobilization is influenced by the properties of the magnetite nanoparticle coating. *J Nanomater* 2018; 2008: 1–9.

16. Arias JL, Reddy LH and Couvreur P. Fe3O4/chitosan nanocomposite for magnetic drug targeting to cancer. *J Mater Chem* 2012; 22: 7622–7632.

17. Lim EK, Sajomsang W, Choi Y, et al. Chitosan-based intelligent theragnosis nanocomposites enable pH-sensitive drug release with MR-guided imaging for cancer therapy. *Nanoscale Res Lett* 2013; 8: 467–512.

18. Yuan Q, Venkatasubramanian R, Hein S, et al. A stimulus-responsive magnetic nanoparticle drug carrier: magnetite encapsulated by chitosan-grafted-copolymer. *Acta Biomater* 2008; 4: 1024–1037.

19. Flores Urquizo IA, García Casillas PE and Chapa González C. Development of magnetic nanoparticles $Fe^{+3}_2 X^{+2}_1 O_4$ (X= Fe, Co y Ni) coated by amino silane. *Mex J Biomed Eng* 2017; 38: 402–411.

20. Scherrer P. Bestimmung der inneren struktur und der größe von kolloidteilchen mittels röntgenstrahlen. In: *Kolloidchemie Ein Lehrbuch*. Berlin, Heidelberg: Springer Berlin Heidelberg, pp. 387–409.

21. Mahadevan S, Gnanaprakash G, Philip J, et al. X-ray diffraction-based characterization of magnetite nanoparticles in presence of goethite and correlation with magnetic properties. *Phys E: Low-dimensional Syst Nanostruct* 2007; 39: 20–25.

22. Blanco-Andujar C, Ortega D, Pankhurst QA, et al. Elucidating the morphological and structural evolution of iron oxide nanoparticles formed by sodium carbonate in aqueous medium. *J Mater Chem* 2012; 22: 12498–12506.

23. Morales-Morales JA. Synthesis of Hematite α-Fe_2O_3 Nano powders by the controlled precipitation method. *Ciencia en Desarrollo* 2017; 8: 99–107.

24. Kibasomba PM, Dhlamini S, Maaza M, et al. Strain and grain size of TiO2 nanoparticles from TEM, Raman spectroscopy and XRD: The revisiting of the Williamson-Hall plot method. *Results Phys* 2018; 9: 628–635.

25. Saleem A, Zhang Y, Gong H, et al. Structural, magnetic and dielectric properties of nano-crystalline spinel NixCu1-xFe2O4. *J Alloys Compounds* 2020; 825: 154017.

26. Gohi BFCA, Zeng H-Y, Xu S, et al. Optimization of ZnAl/chitosan supra-nano hybrid preparation as efficient antibacterial material. *IJMS* 2019; 20: 5705.

27. Banerjee T, Mitra S, Kumar Singh A, et al. Preparation, characterization and biodistribution of ultrafine chitosan nanoparticles. *Int J Pharmaceutics* 2002; 243: 93–105.

28. Lv H-X, Zhang Z-H, Wang X-P, et al. A biomimetic chitosan derivates: preparation, characterization and transdermal enhancement studies of N-arginine chitosan. *Molecules* 2011; 16: 6778–6790.

29. Korolkov IV, Ludzik K, Kozlovskiy AL, et al. Carboranes immobilization on Fe3O4 nanocomposites for targeted delivery. *Mater Today Commun* 2020; 24: 101247.

30. Castrejón-Parga KY, Camacho-Montes H, Rodríguez-González CA, et al. Chitosan-starch film reinforced with magnetite-decorated carbon nanotubes. *J Alloys Compd* 2015; 615: S505–S510.

31. Vidojkovic S, Rodriguez-Santiago V, Fedkin MV, et al. Electrophoretic mobility of magnetite particles in high temperature water. *Chem Eng Sci* 2011; 66: 4029–4035.

32. Favela-Camacho SE, Samaniego-Benítez EJ, Godínez-García A, et al. How to decrease the agglomeration of magnetite nanoparticles and increase their stability using surface properties. *Colloids Surf A: Physicochemical Eng Aspects* 2019; 574: 29–35.

33. Višnjar T and Kreft ME. The complete functional recovery of chitosan-treated biomimetic hyperplastic and normoplastic urothelial models. *Histochem Cel Biol* 2015; 143: 95–107.

34. Ramanery FP, Mansur AA and Mansur HS. One-step colloidal synthesis of biocompatible water-soluble ZnS quantum dot/chitosan nanoconjugates. *Nanoscale Res Lett* 2013; 8: 512.

35. Hong P-Z, Li S-D, Ou C-Y, et al. Thermogravimetric analysis of chitosan. *J Appl Polym Sci* 2007; 105: 547–551.

36. Savliwala S, Chiu-Lam A, Unni M, et al. Magnetic nanoparticles. In: Chung EJ, Lorraine L and Rinaldi C (eds) *Nanoparticles for Biomedical Applications. Fundamental Concepts, Biological Interactions and Clinical Applications. Micro and Nano Technologies*. Oxford: Matthew Deans, 2020; pp. 195–221.